

An Effective Constitutive Model for Lime Treated Soils

V. Robin^{1,2}, A. A. Javadi¹, O. Cuisinier², F. Masrouri²

¹*Computational Geomechanics Group, Department of Engineering, University of Exeter, United-Kingdom*

²*LEMETA – UMR 7563 CNRS, Laboratoire d’Énergétique et de Mécanique Théorique et Appliquée, Université de Lorraine, France*

Abstract

The effect of lime on the yield stress, and more generally the presence of structure in the soil, is usually not accounted for in the design of geotechnical structures. As a result the potential of lime treatment or of a structured soil has not been fully exploited. This paper presents a new formulation to account for the effect of structure on the mechanical behaviour for structured soils. A constitutive model is proposed in the framework of the Modified Cam Clay model to describe the behaviour of lime treated soils. The new formulation introduces a limited number of additional parameters, all of which have a physical meaning and can be obtained from an isotropic compression test. Due to similarity in behaviour of lime treated soils and naturally structured soils, the formulation can be applied to both types of soil. It is shown that the proposed model can successfully reproduce the main features of both structured soils such as maximum rate of dilation at softening and degradation at yield. The model can be applied for any structured material regardless of the origin of cementation.

Keywords:

lime treated soils, structured soils, degradation, constitutive modelling.

1. Introduction

The use of on-site materials has become a central issue for civil engineering companies, but it is sometimes difficult to deal with all the resources available on site. For soils with low mechanical characteristics, lime treatment appears to be an efficient method to improve their mechanical properties and allow their use in geotechnical earth structures (e.g. [Little, 1995](#)). The effects of the addition of lime on the soil parameters such as cohesion and friction angle have been extensively studied (e.g. [Brandl, 1981](#)). Nevertheless, lime is still mostly used to dry soils with high water contents and increase the bearing capacity. However, it is also generally known that adding lime leads to a significant increase of the yield stress and modifies other mechanical parameters in compacted soils. In lime-treated soils, the modification of the mechanical behaviour results from several physico-chemical processes associated with the increase in calcium concentration and pH (i.e. cation exchange, pozzolanic reactions, etc...).

20 From an economical point of view, it is becoming increasingly important to account for the properties
21 of treated materials in the design of the geotechnical structures. However, despite its proven efficacy, the
22 use of treated materials suffers from several major drawbacks: there is no reliable method to account for
23 the structure in the calculations. At yield, and for an increasing mechanical loading, treated materials
24 experience what is called the "loss of structure", resulting in the degradation of the structure in different
25 ways. To model the behaviour of these materials, a constitutive law describing the behaviour at yield is a
26 requirement.

27 Some studies ([Maccarini, 1987](#); [Aversa, 1991](#); [Leroueil and Vaughan, 1990](#); [Liu and Carter, 2003](#); [Flora
28 et al., 2006](#)) have shown that naturally structured soils and artificially treated materials have common
29 mechanical features; artificial treatment appears to create a "structure" in the soil. In this paper, "structure"
30 refers to Burland's definition ([Burland, 1990](#)), and is seen as the combination of the fabric and the bonding of
31 the soil skeleton. Fabric accounts for the arrangement of particles, which depends on the state of compaction
32 and their geometry.

33 Several constitutive models have been proposed for structured materials. Most of these models use the
34 destructured state as reference to describe the mechanical behaviour of structured soils. [Liu and Carter
35 \(2002\)](#) proposed a constitutive model, based on the Modified Cam Clay model (MCC), by adding three
36 additional parameters to the original MCC ([Roscoe and Burland, 1968](#)). Since then, several enhancements
37 (e.g. [Horpibulsuk et al., 2010](#); [Suebsuk et al., 2011](#)) have been proposed. However, various modes of de-
38 structuration have been identified, and the original formulation fails to model some of them. A number
39 of other formulations have been developed ([Kavvasdas and Amorosi, 2000](#); [Vatsala et al., 2001](#); [Nova et al.,
40 2003](#); [Baudet and Stallebrass, 2004](#); [Rouainia and Muir wood, 2000](#); [Nguyen et al., 2014](#)) and some of which
41 give good agreement with experimental results. However, it often comes at the cost of a larger number of
42 parameters, or high computational resources (e.g. mapping rule). Parameters do not always have a physical
43 meaning, and some of them can be difficult to determine. All these limitations make these models difficult
44 to be used in engineering practice.

45 The main objective of this paper is to propose a general and simple formulation capable of fulfilling some
46 fundamentals criteria regarding the degradation of the structure. This model must be capable of modelling
47 any kind of degradations, and require a limited number of parameters to account for the maximum number
48 of features of structured materials. These parameters should be rapidly obtained from classic experimental
49 tests, and they all must have a physical meaning. To this end, the paper will focus on two aspects:

- 50 • How can the key features of structured or lime treated materials be described?
- 51 • How can these features be efficiently accounted for in a constitutive model?

52 This paper is divided into four parts. The first part gives a review of the main characteristics of naturally
53 and artificially structured materials that must be reproduced by the model. The second part introduces the

54 theoretical framework chosen for the model for lime treated soils (MLTS) and the new formulation developed
55 to model the degradation of the structure. In the third part, the developed formulation is used to calculate
56 the compliance matrix and obtain the stress-strain relationship. Finally, in the last part, we assess the
57 suitability of the model in predicting experimental results obtained from triaxial tests on artificially (i.e.
58 lime treated) and naturally structured materials.

59 2. Features of structured soils

60 The mechanical behaviour of naturally and artificially structured material has been extensively studied
61 (Leroueil and Vaughan, 1990; Gens and Nova, 1993; Burland et al., 1996; Cotecchia and Chandler, 2000;
62 Malandraki and Toll, 2001; Cuisinier et al., 2008, 2011; Consoli et al., 2011; Oliveira, 2013; Robin et al.,
63 2014a) and some specific features have been identified. Several studies have pointed out that naturally and
64 artificially structured soils have a similar mechanical behaviour. In this section, we identify the key features
65 common to naturally and artificially structured soils that should be properly reproduced by a model.

66 2.1. Naturally structured soils

67 It has been shown that naturally structured soils have a higher yield stress compared to the destructured
68 state (Burland et al., 1996), the latter being usually considered as the reference state. For the same stress
69 state, a higher yield stress leads to a higher void ratio at yield compared to the destructured state, called
70 the additional void ratio Δe . Once plastic deformations take place, one can observe that the additional
71 void ratio decreases. Depending on the material, the additional void ratio can quickly or slowly decrease
72 until the material reaches a normal compression line (ncl), which can correspond to the ncl of the reference
73 state (ncl_d), or a different one, parallel to the reference ncl but vertically translated along the v axis (ncl_r)
74 (Baudet and Stallebrass, 2004; Callisto and Rampello, 2004; Suebsuk et al., 2011). More generally, 4 modes
75 of degradation can be identified (Figure 1):

76 **Mode 1:** Destructuration takes place immediately at yield. The additional void ratio progressively de-
77 creases until it converges toward the destructured state (Yong and Nagaraj, 1977; Lagioia and Nova,
78 1995).

79 **Mode 2:** Destructuration takes place immediately at yield, but it does not converge toward its destructured
80 state. A different ncl appears parallel to the destructured state, but a residual additional void ratio
81 still remains (Burland et al., 1996; Rampello and Callisto, 1998).

82 **Mode 3:** No significant destructuration is observed immediately after yield. The process of degradation is
83 initiated later on for a higher effective mean stress and the additional void ratio completely disappears
84 (Callisto and Rampello, 2004).

85 **Mode 4:** No destructuration is observed immediately after yield. The process of degradation is initiated
 86 later on for a higher effective mean stress. However, a residual additional void ratio remains (Rotta
 87 et al., 2003).

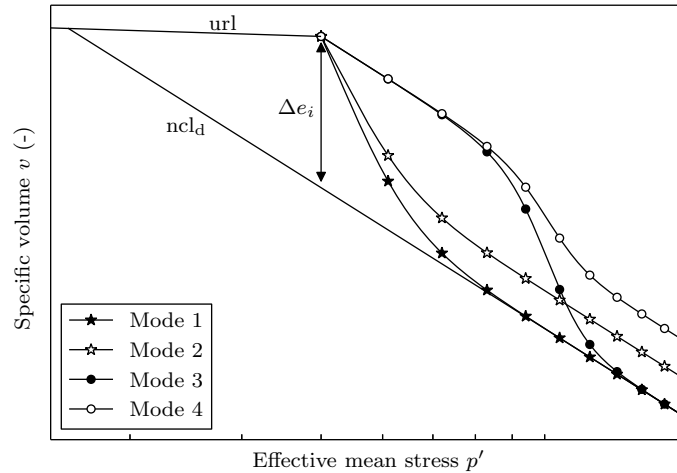


Figure 1: The four different modes of destructuration in structured soils – ncl_d: Normal compression line of the destructured state, url: Unloading-reloading line.

88 Additionally, the volumetric behaviour of naturally structured soils was compared with the destructured
 89 state by Leroueil and Vaughan (1990) on heavily overconsolidated specimens from drained triaxial test
 90 results. They identified two different mechanisms taking place. While the maximum rate of dilation was
 91 measured before the peak of the deviatoric stress for the destructured soil, it was observed after the peak
 92 of the deviatoric stress for structured soils. This is due to the structure, which binds soil particles together.
 93 To allow the particles to move freely, the structure has to be degraded first to release particles (Leroueil and
 94 Vaughan, 1990).

95 2.2. Lime treated soils

96 Several studies have shown that addition of lime leads to an increase of the yield stress compared to the
 97 untreated state (Tremblay et al., 2001; Ahnberg, 2007). As for naturally structured soils, the additional void
 98 ratio appears to decrease at yield, i.e. the degradation of the artificial structure takes place. Robin et al.
 99 (2014a) have assessed the mechanical behaviour of a lime treated silt under isotropic loading (Figure 2). It
 100 can be seen that the mode of degradation depends on the amount of lime. For 0.5% in lime, the additional
 101 void ratio completely disappears at high stress states (Mode 3), when it is not the case for 1% lime treated
 102 specimens (Mode 4). This latter reaches a different ncl compared to the untreated specimen. Details about
 103 the samples and experimental conditions can be found in Robin et al. (2014a).

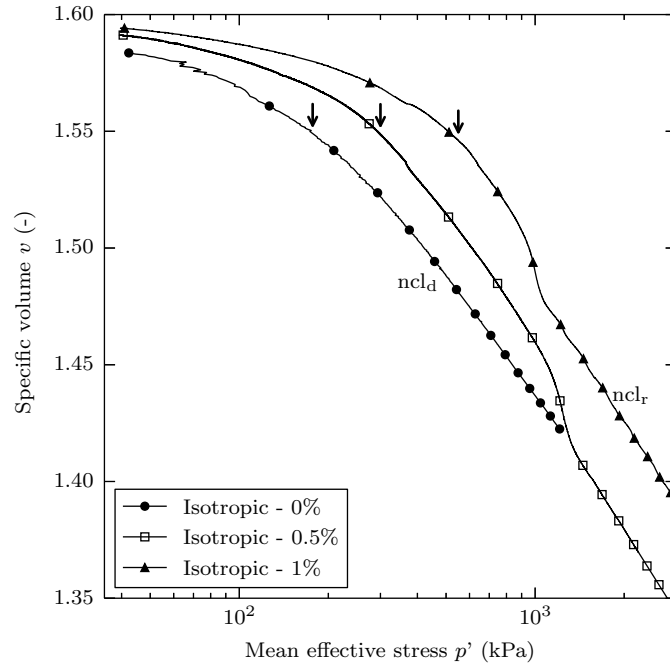


Figure 2: Isotropic consolidation curves obtained from specimens of silt treat at 0.5% and 1% in lime – Arrows mark the yield stress p'_y , ncl_d : Normal compression line of the destructured state, ncl_r : Normal compression line of the residual state (Robin et al., 2014a).

104 The maximum rate of dilation at shear for specimens experiencing softening also appears after the
 105 peak for artificially structured soils, which indicates that the same kind of mechanism is taking place. This
 106 common feature was pointed out by Leroueil and Vaughan (1990), and was also observed for the lime treated
 107 specimens from the current study (Figure 3).

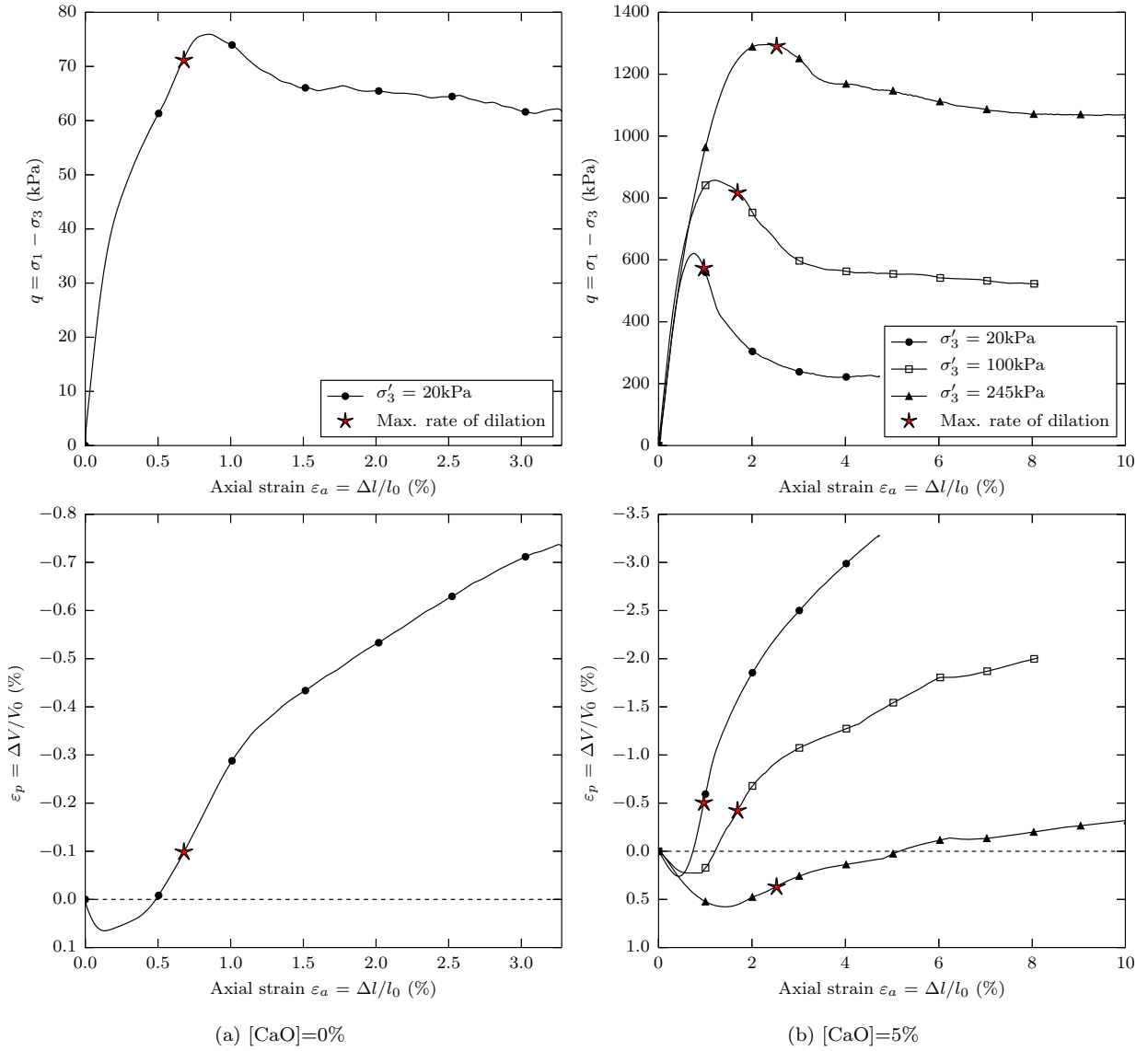


Figure 3: Drained triaxial results on (a) untreated and (b) lime treated soils – Stars mark the location where the rate of dilation is maximum (Robin et al., 2014a).

108 The influence of a lime treatment on the cohesion and the friction angle has been studied by several
 109 authors (Wissa et al., 1965; Balasubramaniam et al., 2005). Both cohesion and friction angle appear to
 110 increase with the amount of lime. The slope of the critical state line is directly related to the friction angle,
 111 and the increase of cohesion, which increases the tensile strength, has an influence on the shape of the yield
 112 function. Therefore, in the framework the critical state theory, these features should be accounted for in the
 113 model.

114 2.3. Summary

115 Based on the previous observations, a model for lime treated soils might be suitable for naturally struc-
116 tured soils, and therefore should be able to reproduce the four modes of destructureation and account for the
117 following features:

- 118 • The cohesion increases following pozzolanic reactions,
- 119 • The yield stress increases for lime treated soils compared to the reference state,
- 120 • At yield, there exists an additional void ratio compared to the reference state,
- 121 • At yield, degradation of the structure takes place, which follows one of the four modes identified
122 previously,
- 123 • Overconsolidated specimens at shear show a maximum rate of dilation after the peak, describing the
124 degradation of the structure,
- 125 • The friction angle is modified due to the effects of the chemical reactions on the texture of the soil,
126 and therefore the critical state as well.

127 3. Theoretical framework of the model

128 The model proposed in this paper was developed in the framework of the Modified Cam Clay model
129 (MCC) to model the key features of lime treated soils previously identified. The new parameters introduced
130 to model the degradation have all a physical meaning and can be determined from an isotropic compression
131 test (Robin et al., 2014b). We present in this section a new formulation to model the four modes of
132 degradation in structured soils under isotropic loading. This will then be used as a hardening rule for the
133 determination of the compliance matrix.

134 3.1. Modelling the structure and its degradation under isotropic loading

135 To model the degradation of the structure under isotropic loading, we propose the framework given
136 in Figure 4. We introduce the *primary yield stress* p_y^I , which corresponds to the apparition of plastic
137 deformations. To describe the stress states for which the degradation of the structure takes place (hatched
138 area in Figure 4), we also introduce the *degradation stress* p_y^{II} . In the case of an immediate degradation
139 of the structure at yield (modes 1 & 2 in Figure 1), which can happen for some structured soils, we have
140 $p_y^{II} = p_y^I$. The additional void ratio Δe_i at p_y^I quantifies the initial additional void ratio at yield. Δe_c is
141 measured at an effective mean stress above which the additional void ratio remains constant ($p' \gg p_y^{II}$).
142 By setting the parameters as given in Table 1, this framework is capable of describing the four modes of
143 degradation.

144 In this study, the structure is quantified through the additional void ratio in comparison to the ncl_d and
 145 is assumed to be made of two components. The first one, referred to as the *available structure*, corresponds
 146 to the part of structure that will be available during the process of destructuration ($\Delta e_i - \Delta e_c$). The
 147 second one, referred to as the *residual structure*, corresponds to the persisting additional void ratio at high
 148 effective mean stress (Δe_c at $p' \gg p_y^I$). The latter can be the consequences of chemical reactions, e.g. a lime
 149 treatment, which leads to a permanent modification of the fabric of the soil (Robin et al., 2014a).

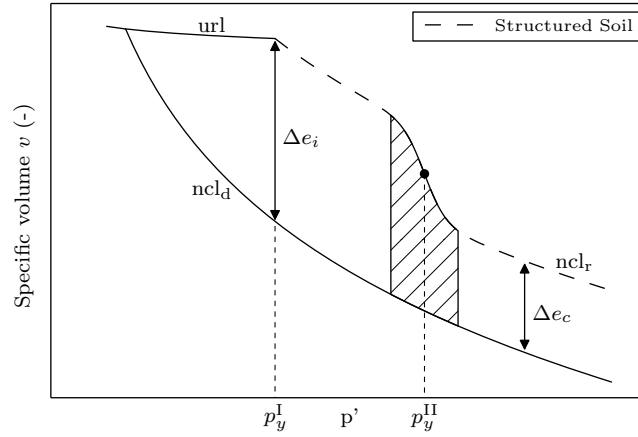


Figure 4: General framework of the degradation of structured soils – Δe_i : Initial additional void ratio, Δe_c : Residual additional void ratio, p_y^I : Primary yield stress, p_y^{II} : degradation stress, hatched area: degradation of the structure, ncl_d : Normal compression line of the destructured state, ncl_r : Normal compression line of the residual state, url: Unloading-reloading line.

Table 1: Conditions on the parameters p_y^{II} and Δe_c for the 4 modes of degradation

Parameters	Values			
	Mode 1	Mode 2	Mode 3	Mode 4
p_y^{II}	p_y^I	p_y^I	$> p_y^I$	$> p_y^I$
Δe_c	0	> 0	0	> 0

150 3.1.1. Mathematical Formulation

To model these four mechanisms, a flexible formulation using all the parameters previously introduced is required. Richards's equation (Richards, 1959) for the sigmoid provides many degrees of freedom to control the shape of the function. This function is frequently used for the modelling natural phenomena where there exists a threshold above which a process is activated, in this case the degradation. This equation can be written as follows:

$$\forall p' \in [p_y^I, +\infty[\quad \pi(p') = 1 - \frac{1}{1 + e^{-\beta(p' - p_y^{II})}} \quad (1)$$

151 where p_y^{II} [Pa] corresponds to the position of the inflection point ($\pi''(p_y^{\text{II}}) = 0$) and describes the stress
 152 state for which the degradation occurs (hatched area in Figure 4), and β [Pa^{-1}] describes the rate of
 153 degradation.

Therefore, we have

$$\forall p' \in \mathbb{R} \quad 0 \leq \pi(p') \leq 1 \quad (2)$$

154 3.1.2. Scaling of π

The function π is scaled to ensure that $\forall \beta, \forall p_y^{\text{II}} \quad \pi(p_y^{\text{I}}) = 1$, which leads to the following final formulation:

$$\forall p' \in [p_y^{\text{I}}, +\infty[\quad \pi(p') = \frac{e^{\beta p_y^{\text{I}}} + e^{\beta p_y^{\text{II}}}}{e^{\beta p'} + e^{\beta p_y^{\text{II}}}} \quad (3)$$

155 which verifies $\pi(p_y^{\text{I}}) = 1$ and $\lim_{p' \rightarrow +\infty} \pi(p') = 0$.

156 The ability to control the rate of degradation at yield of this formulation is demonstrated in Figure 5. It
 157 can be seen that the function π can either slowly decrease with a low β or quickly with a high β as p' gets
 158 close to p_y^{II} .

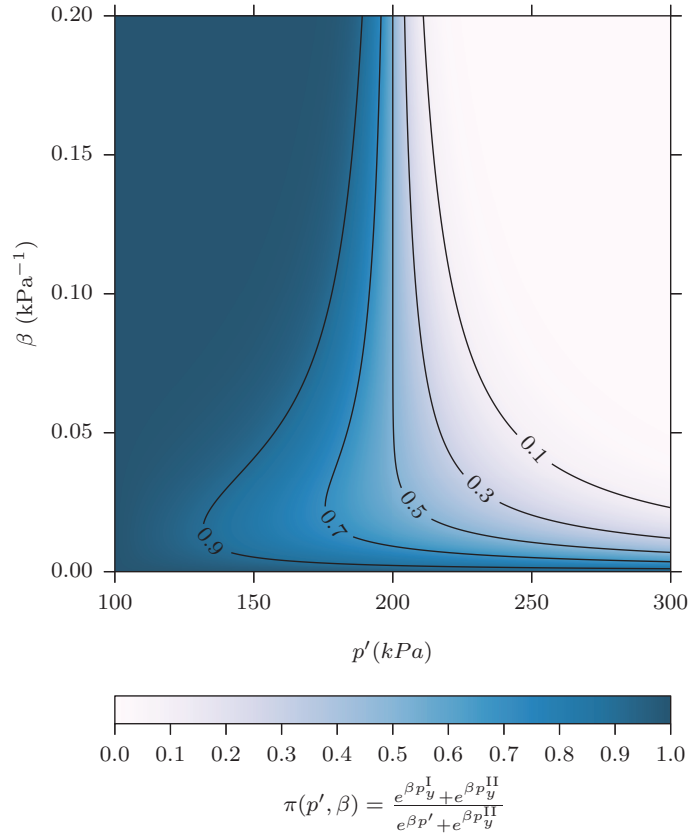


Figure 5: π values as a function of p_y^{II} and $\beta - p_y^{\text{I}}=100$ kPa, $p_y^{\text{II}}=200$ kPa.

159 *3.1.3. Relationship between the specific volume and the effective mean stress for structured soils*

The presence of structure can be accounted for in the relationship between the specific volume and the effective mean stress ($v : p'$ relationship) using the following general formulation:

$$\forall p' \in \mathbb{R}_+^* \quad v(p') = N_\lambda - \lambda \ln(p') + \Delta e(p') \quad (4)$$

160 with N_λ the intercept on the reference normal compression line ncl_d and λ the slope of the reference ncl
 161 in $v : \ln(p')$ plane.

162 Using the function π (Equation 3), the equation for the additional void ratio is given by:

$$\forall p' \in [p_y^I, +\infty[\quad \Delta e(p') = (\Delta e_i - \Delta e_c) \cdot \left[\frac{e^{\beta p_y^I} + e^{\beta p_y^{II}}}{e^{\beta p'} + e^{\beta p_y^{II}}} \right] + \Delta e_c \quad (5)$$

which fulfils the boundary value problems:

$$\Delta e(p') = \begin{cases} \Delta e_i & \text{if } p' = p_y^I \\ \Delta e_c & \text{if } p' \rightarrow +\infty \end{cases} \quad (6)$$

Introducing Equation 5 in Equation 4 gives the final equation of the specific volume for structured soils at yield:

$$\forall p' \in [p_y^I, +\infty[\quad v_s(p') = N_\lambda - \lambda \ln(p') + (\Delta e_i - \Delta e_c) \cdot \left[\frac{e^{\beta p_y^I} + e^{\beta p_y^{II}}}{e^{\beta p'} + e^{\beta p_y^{II}}} \right] + \Delta e_c \quad (7)$$

163 *3.1.4. Determination of β*

164 β can be directly determined from the results of an isotropic compression test. Practically, β is related
 165 to the gradient ξ on the $v : p'$ curve at $p' = p_y^{II}$ (Figure 6). For consistency and stability, the function v_s for
 166 the specific volume in the $v : p'$ plane must be strictly monotonic decreasing on $[p_y^I, +\infty[$, which imposes
 167 $\beta \geq 0$.

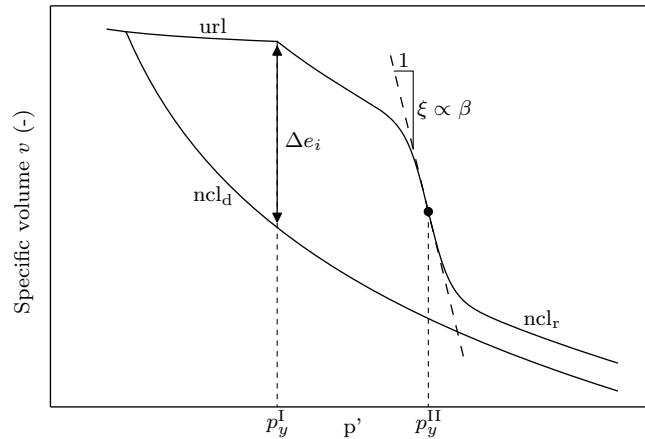


Figure 6: Physical meaning of β – ncl_d : Normal compression line of the destructured state, ncl_r : Normal compression line of the residual state, url : Unloading-reloading line.

Calling ξ the gradient of the specific volume curve at $p' = p_y^{\text{II}}$, the appropriate value for β is obtained by solving the following equation:

$$\left(\frac{dv}{dp'}\right)_{p'=p_y^{\text{II}}} = \xi \Leftrightarrow -\frac{1}{4} \left(1 + e^{\beta(p_y^{\text{I}} - p_y^{\text{II}})}\right) \times \beta(\Delta e_i - \Delta e_c) - \frac{\lambda}{p_y^{\text{II}}} = \xi \quad (8)$$

168 There is no analytical solution to this equation, known as the Lambert W function, due to the non-
 169 linearity in β . However, this equation can be solved graphically or numerically using methods such as the
 170 Newton-Raphson algorithm (Corless et al., 1996).

171 3.1.5. Suitability of the formulation

172 The $v : p'$ relationship (Equation 7) is used to demonstrate the ability of the formulation to describe
 173 the four modes (Figure 7). Parameters used for the simulations are given in Table 2. The influence of
 174 the parameters β (Figure 8) and the degradation stress p_y^{II} (Figure 9) is assessed and the case $p_y^{\text{I}} = p_y^{\text{II}}$ is
 175 considered in Figure 10.

176 Figure 8 shows that it is possible to describe the mode 3. Changing the value of β permits to achieve
 177 different rates of degradation. In this figure, a non-zero Δe_c was chosen ($\Delta e_c > 0$), but mode 4 can be
 178 achieved by setting $\Delta e_c = 0$. The influence of p_y^{II} is shown in Figure 9. One can see that this parameter
 179 controls the initiation of the process of degradation, and is successful in describing modes 2 and 4. As
 180 previously, modes 1 and 3 can be achieved by setting $\Delta e_c = 0$. Finally, the case $p_y^{\text{I}} = p_y^{\text{II}}$ is considered in
 181 Figure 10. This case corresponds to an immediate loss of structure at yield. This case does not lead to any
 182 instabilities of the formulation.

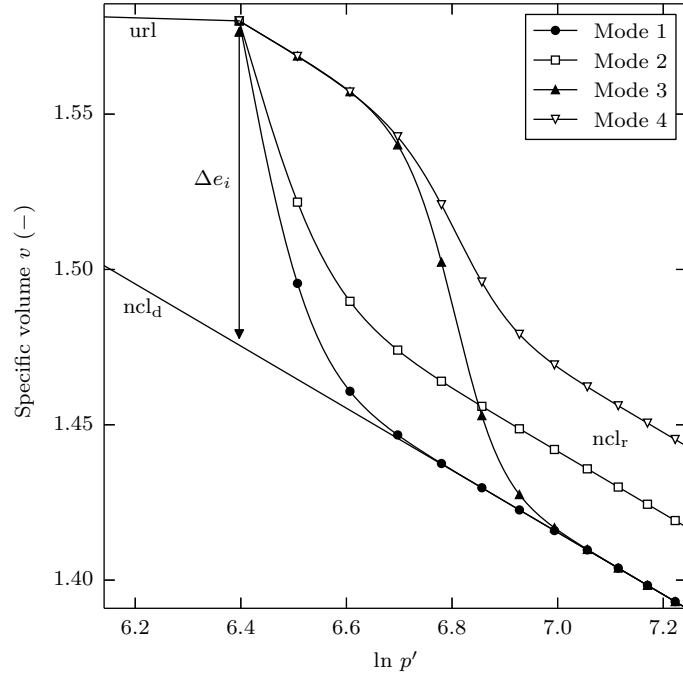


Figure 7: Possibility of the formulation to model the four modes – ncl_d : Normal compression line of the untreated state, url : Unloading-reloading line.

Table 2: Model parameters used for simulations of the four modes in Figure 7

Mode	p_y^I (kPa)	p_y^{II} (kPa)	Δe_i	Δe_c	β (kPa $^{-1}$)
Mode 1	600	600	0.104	0.0	0.025
Mode 2	600	600	0.104	0.026	0.02
Mode 3	600	900	0.104	0.0	0.025
Mode 4	600	900	0.104	0.052	0.02

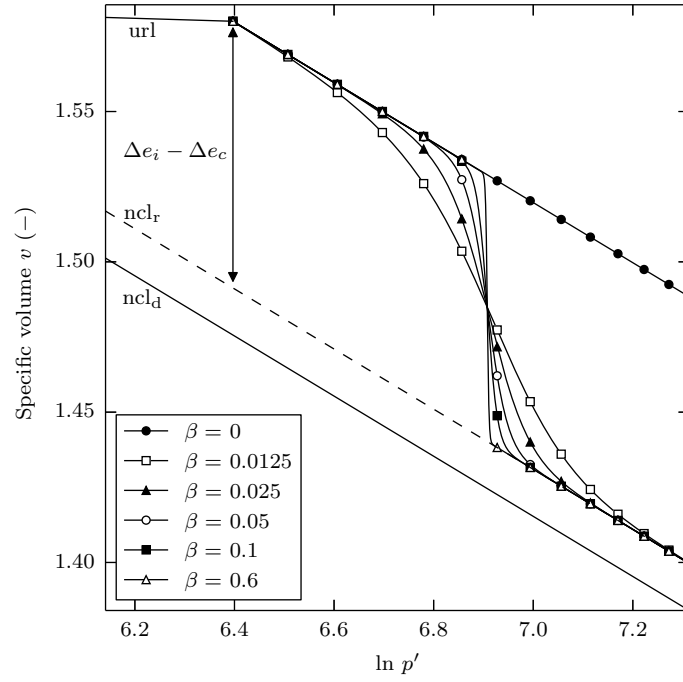


Figure 8: Influence of β : $p_y^I = 600$ kPa, $p_y^{II} = 1000$ kPa, $\Delta e_c > 0$ – Mode 4.

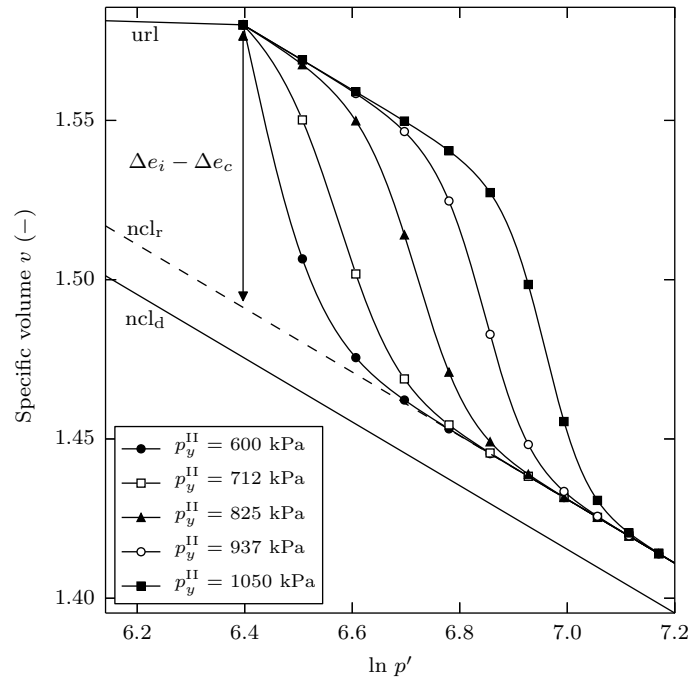


Figure 9: Influence of p_y^{II} : $p_y^I = 600$ kPa, $\beta = 0.025$, $\Delta e_c > 0$ – Modes 2 and 4.

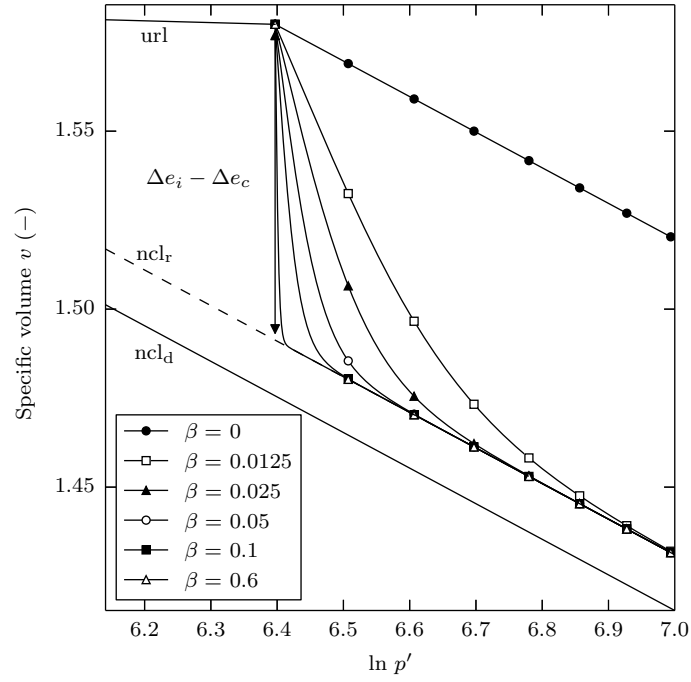


Figure 10: Influence of β : $p_y^{\text{II}} = p_y^{\text{I}} = 600$ kPa, $\Delta e_c > 0$ – Mode 2.

183 3.2. Yield function f

184 The addition of lime leads to an increase of the cohesion and the friction angle compared to the untreated
 185 soil. Therefore, the equation of the MCC for the yield function f is not sufficient in its original form. One
 186 way to account for the increase of cohesion is to consider it as an increase of the tensile strength (e.g.
 187 Suebsuk et al. (2010)). This can be modelled by expanding the yield function in the negative stress domain
 188 (Figure 11). The parameter p_b (< 0) is introduced to control the expansion of the yield function due to the
 189 increase of the cohesion and is directly obtained from the equation of the CSL. The critical state line does
 190 not necessarily pass through the origin anymore.

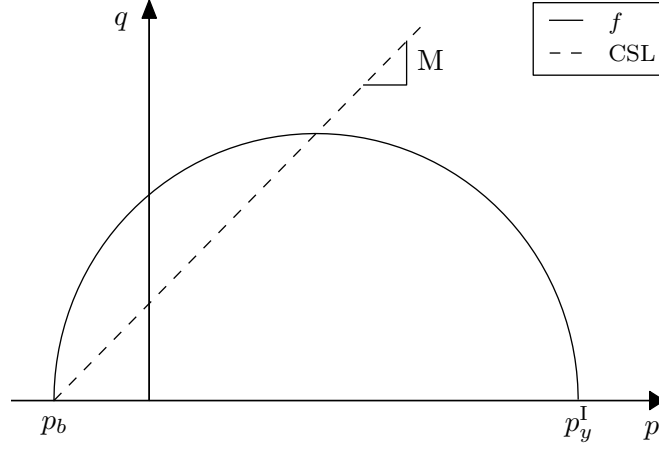


Figure 11: Theoretical yield function for lime treated soils.

The equation chosen for the yield function can therefore be expressed as:

$$f \equiv q^2 + M^2(p' - p_y^I)(p' - p_b) \equiv 0 \quad (9)$$

191 3.3. Plastic potential g

The choice of the formulation for the plastic potential g is a major issue in the constitutive modelling of soils. The use of non-associated potentials gives a more accurate description of the real behaviour but comes at the cost of additional parameters with, in most of the cases, no straightforward physical meaning and whose values can rarely be determined from experimental results. This study aims to develop a model based on meaningful parameters determined from classic experimental tests. To this end, always in the framework of the Modified Cam Clay model, this model assumes that lime treated materials follow an associated flow rule and therefore

$$g \equiv f \quad \Rightarrow \quad g \equiv q^2 + M^2(p' - p_y^I)(p' - p_b) \quad (10)$$

which leads to the following flow rule for lime treated materials:

$$\frac{\delta \varepsilon_p^p}{\delta \varepsilon_q^p} = \frac{\partial g / \partial p'}{\partial g / \partial q} = \frac{M^2(p' - p_b)}{2p'\eta} - \frac{p'\eta}{2(p' - p_b)} \quad (11)$$

192 with $\eta = q/p'$. The suitability of this hypothesis will be verified in the [Model evaluation](#) section.

193 3.4. Summary of the model parameters

194 Using the sigmoid equation, a new formulation has been developed to model the degradation of structure
 195 at yield for lime treated soils (Equation 7). This formulation has the significant advantage to rely on only
 196 4 additional parameters to the original MCC (β , p_y^{II} , Δe_i and Δe_c), which all have a physical meaning and
 197 can all be determined from an isotropic consolidation test performed on the lime treated material. To model

198 the influence of the cohesion on the deviatoric behaviour the parameter p_b , directly related to the equation
 199 of the CSL, was introduced. As a conclusion, the following 6 parameters appear to be relevant to account
 200 for the effects of a lime treatment on the mechanical behaviour of a material:

201

- p_y^I : Primary yield stress
- p_y^{II} : Degradation stress
- Δe_i : Additional void ratio at p_y^I
- 202 Δe_c : Additional void ratio for $p' \rightarrow +\infty$
- β : Rate of degradation
- p_b : Tensile strength due to the increase of the cohesion

203 4. Stress-strain relationship

204 4.1. Elastic behaviour

It is assumed that only elastic deformation occurs for stress states lying within the yield surface. According to the Modified Cam Clay model, the elastic volumetric increments are given by

$$\delta \varepsilon_p^e = \kappa \frac{\delta p'}{v p'} \quad (12)$$

$$\delta \varepsilon_q^e = \frac{\delta q}{3G} \quad (13)$$

205 with G the shear modulus. As recommended by several authors (e.g. [Liu and Carter \(2002\)](#); [Muir Wood](#)
 206 [\(2004\)](#)), Poisson's ratio ν is assumed constant in this model, although it is known to lead to thermodynamic
 207 discrepancies under cyclic loading ([Zytynski et al., 1978](#)).

208 4.2. Plastic behaviour

209 4.2.1. Compliance matrix for hardening case

The general plastic stress:strain relationship is given by

$$\begin{bmatrix} \delta \varepsilon_p^p \\ \delta \varepsilon_q^p \end{bmatrix} = \frac{-1}{\left[\frac{\partial f}{\partial p'_0} \left[\frac{\partial p'_0}{\partial \varepsilon_p^p} \frac{\partial g}{\partial p'} + \frac{\partial p'_0}{\partial \varepsilon_q^p} \frac{\partial g}{\partial q} \right] \right]} \begin{bmatrix} \frac{\partial f}{\partial p'} \frac{\partial g}{\partial p'} & \frac{\partial f}{\partial q} \frac{\partial g}{\partial p'} \\ \frac{\partial f}{\partial p'} \frac{\partial g}{\partial q} & \frac{\partial f}{\partial q} \frac{\partial g}{\partial q} \end{bmatrix} \begin{bmatrix} \delta p' \\ \delta q \end{bmatrix} \quad (14)$$

210 The new formulation of the $v : p'$ relationship given by Equation (7) is now used as the new hardening
 211 rule. For the sake of simplicity, it was assumed that hardening is only controlled by the plastic volumetric
 212 strains ($f(\boldsymbol{\sigma}, \varepsilon_p^p)$). The volumetric plastic strains for lime treated soils is therefore expressed as

$$\delta\varepsilon_p^p = \left[\left(\frac{M^2(2p' - p'_0 - p_b) + 6q}{M^2(p' - p_b)} \right) \left(\frac{\partial p'_0}{\partial \varepsilon_p^p} \right)^{-1} \right] \cdot \delta p' \quad (15)$$

and the deviatoric plastic strains can be calculated using the flow rule:

$$\delta\varepsilon_q^p = \left[\frac{M^2(p' - p_b)}{2p'\eta} - \frac{p'\eta}{2(p' - p_b)} \right]^{-1} \cdot \delta\varepsilon_p^p \quad (16)$$

213 4.2.2. Compliance matrix for softening case

214 Lime treated specimens experiencing softening at shear show a maximum rate of dilatation after the
 215 peak due to the degradation of the structure. The modelling of these features without introducing additional
 216 parameters is a delicate issue. The Structure Cam Clay model (Liu and Carter, 2002) has a formulation for
 217 the softening case, but which can lead to contraction of the material at softening. More recently Yang et al.
 218 (2014) have proposed a simple formulation based on the SCCM, but although promising does not lead to
 219 accurate predictions of the behaviour.

220 If Equation (5) is used to model the softening behaviour on $]0, p_y^I]$, the formulation leads to $\Delta e \geq \Delta e_i$
 221 and no degradation of the structure is modelled. To model the softening behaviour, we propose a new
 222 softening rule in the same framework as the one chosen for the hardening case, where the degradation of
 223 the structure is described by the sigmoid equation. To avoid the addition of meaningless parameters, an
 224 automatic procedure is proposed based on experimental considerations.

Since Δe_c arises from the lime treatment and modifies the texture of the soil, it is assumed that the material converges toward the same n_{cl_r} as under isotropic loading. Based on experimental observations (Robin et al., 2014a) the inflexion point, called $p_{y,s}^{II}$, was chosen as the intersection of the url and the n_{cl_r} (Figure 12) and is given by

$$p_{y,s}^{II} = \exp \left(\frac{N_\lambda - N_\kappa + \Delta e_c}{\lambda - \kappa} \right) \quad (17)$$

which does not require any additional parameter. This leads to the following expression of the softening rule:

$$\forall p' \in]0, p_y^I] \quad v_s(p') = N_\lambda - \lambda \ln(p') + (\Delta e_i - \Delta e_c) \cdot \left[\frac{e^{-\beta_s p_y^I} + e^{-\beta_s p_{y,s}^{II}}}{e^{-\beta_s p'} + e^{-\beta_s p_{y,s}^{II}}} \right] + \Delta e_c \quad (18)$$

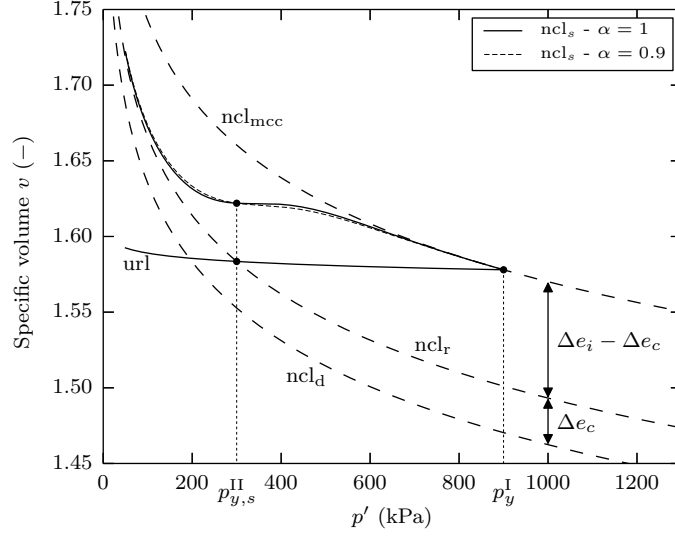


Figure 12: Modelling of the behaviour at yield for softening case.

The parameter β_s describes the rate of destructuration and is calculated automatically. During the post-yield behaviour, the maximum rate of dilation is observed right after the deviatoric stress reaches its maximum. This is due to the structure experiencing an extensive degradation. Such feature can be modelled by using as β_s , the maximum rate of degradation β_0 , leading to v_s monotonically decreasing (not strictly). In this case, the first derivative being zero only for a single effective mean stress (which is not necessarily $p_{y,s}^{II}$). This method presents the advantage that β_0 can easily be determined graphically or numerically. However, for consistency and numerical stability, v_s is preferred to be strictly monotonic decreasing on $]0, p_y^I]$. For this purpose, we introduced a constant α such that

$$\beta_s = \alpha \times \beta_0 \quad (19)$$

225 the bijection (one-to-one correspondence) being ensured by $\alpha \in]0, 1[$. Practically, α can control the
 226 smoothness of the process of destructuration. In this model, α is arbitrarily set to 0.9, which ensures a
 227 bijective function and an appropriate rate of degradation at yield (Figure 12).

228 This two-step method is the simplest and most reliable way to calculate β_s , simply because the deter-
 229 mination of β_0 is independent of the stress state and does not require information about the gradient at
 230 $p_{y,s}^{II}$, which can not be determined from experimental results, and may lead to numerical instabilities. The
 231 suitability of this method will be demonstrated during the [Model evaluation](#) section.

232 The strain-strain relationship for the softening case is obtained by introducing Equation 18 into Equa-
 233 tion 14. Such softening rule respects the associated potential hypothesis.

234 **5. Model evaluation**

235 The robustness of the model for lime treated soils (MLTS) is assessed in predicting the behaviour of
 236 artificially and naturally structured materials under isotropic loading and drained paths for different con-
 237 fining pressures. As a first step, we assess the suitability of an associated flow rule for the modelling of lime
 238 treated soils using the experimental results from Robin et al. (2014a). Then, the model is used to predict
 239 the behaviour of silt specimens treated with different lime contents (0.5%, 1%, 2%, and 5% CaO) (Robin
 240 et al., 2014a). The model is finally tried out on naturally structured specimens of calcarenite (Lagioia and
 241 Nova, 1995). For both cases, the additional parameters to the Modified Cam Clay were determined from a
 242 single isotropic compression test performed on the structured specimens (Table 3).

Table 3: Values of the model parameters

Parameters		[CaO]				Calcarenite
		Robin et al. (2014a)				Lagioia and Nova (1995)
		0.5%	1%	2%	5%	
MCC	p_y^I (kPa)	255	600	1260	1900	2300
	N_λ (-)	1.95	1.99	1.97	2.00	3.76
	λ (-)	0.08	0.08	0.08	0.08	0.23
	κ (-)	0.019	0.032	0.014	0.015	0.020
	M (-)	-	1.15	1.22	1.42	1.42
	E (kPa)	-	45000	55000	70000	77000
MLTS	p_y^{II} (kPa)	1200	1000	2200	3500	2300
	Δe_i (-)	0.027	0.065	0.129	0.159	0.134
	Δe_c (-)	0.0	0.046	0.109	0.136	0.0
	p_b (kPa)	-	-41.8	-120.3	-144.7	-25.6
	β (kPa ⁻¹)	0.020	0.035	0.020	0.020	0.047

MCC: Modified Cam Clay model, MLTS: Model for Lime Treated Soils.

243 *5.1. Associated flow rule hypothesis*

244 In this section, we assess the validity of an associated flow rule for lime treated soils. Plastic strain
 245 increment vectors from drained triaxial tests performed on specimens treated with 1%, 2%, and 5% in
 246 lime were determined. The yield loci values were normalized with respect to the primary yield stress p_y^I .

247 Figure 13 shows that it seems reasonable to assume that plastic strain increment vectors are normal to
 248 the yield surface. The hypothesis of an associated flow rule for the modelling of lime treated soils appears
 249 therefore suitable.

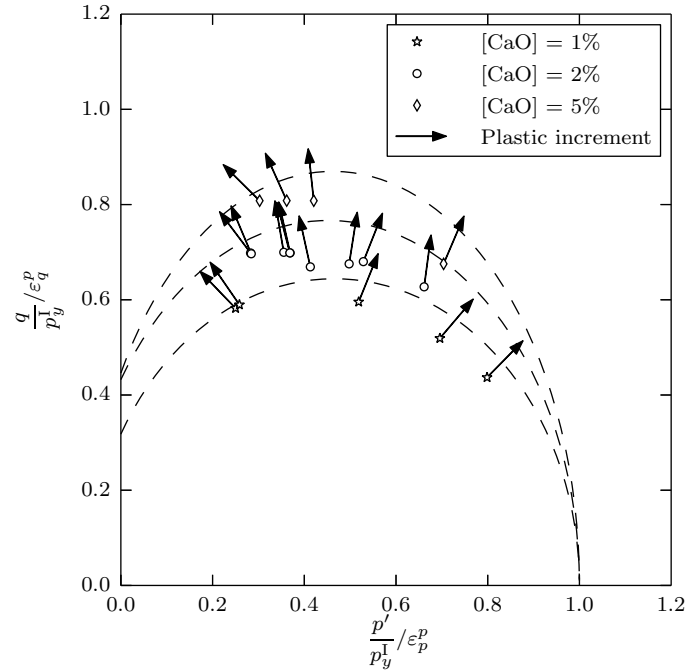


Figure 13: Vectors of plastic strain increment plotted at yield points obtained from drained triaxial tests on lime treated specimens.

250 5.2. Lime treated specimens

251 5.2.1. Isotropic consolidation

252 The new formulation to model the degradation of the structure at yield (Equation 7) was applied on
 253 lime treated specimens. Two sets of experimental results of isotropic compressions tests were used to verify
 254 the general nature of the formulation. The first set was treated with 0.5% CaO and follows the mode 3
 255 ($\Delta e_c = 0$), and the second with 1% CaO and follows the mode 4 ($\Delta e_c > 0$) (Figure 14). For the two sets the
 256 parameter β was determined from the gradient of the curve at $p' = p_y^{\text{II}}$ using the Newton-Raphson algorithm.

257 The use of the sigmoid equation appears very appropriate to model the degradation experienced at yield
 258 by lime treated materials. For both concentrations in lime, there is a very good agreement between the
 259 experimental results and the model. The degradation is initiated at the right effective mean stress and with
 260 the correct rate, and both sets converge toward the correct normal compression line.

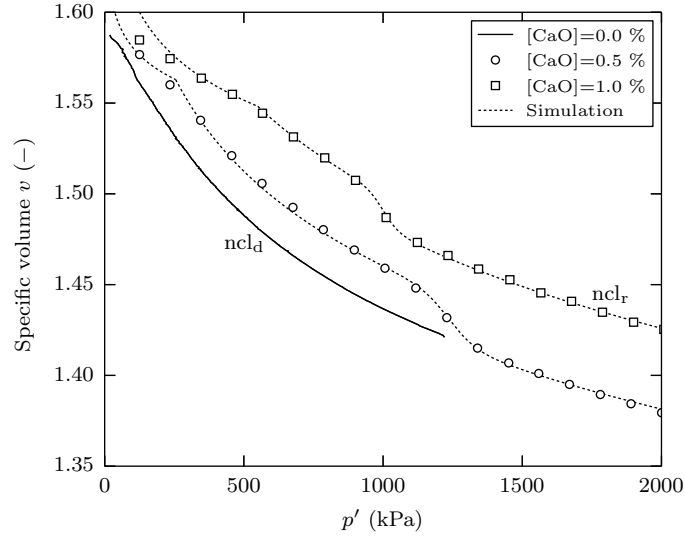


Figure 14: Validation of the formulation on 0.5% and 1% lime treated specimens – ncl_d : normal compression line of the untreated state, ncl_r : normal compression line of the residual state.

261 5.2.2. Shear behaviour

262 No additional parameters to the MCC are required by this model to describe the degradation of the
 263 structure at shear apart from p_b that is derived from the equation of the CSL. The model was applied on
 264 lime treated specimens along different drained stress paths and confining pressures (Figures 15-17). Three
 265 concentrations in lime were tested to consider various degrees of structure: 1%, 2% and 5% CaO.

266 The yield loci and the convergence toward the critical state appear satisfactory modelled for all the lime
 267 contents tested. They confirm the appropriateness of the equation of the yield function f and the suitability
 268 of the parameter p_b to account for the influence of the lime treatment on the cohesion and the critical state.

269 For both hardening and softening cases, the volumetric deformations are very accurately predicted by
 270 the model. This supports the assumption of the volumetric deformations being mostly controlled by the
 271 structure. The evolution of the specific volume for the softening case is particularly accurate (Figure 18).
 272 The model is successful to reproduce the dilation post-yield of the specimens and the maximum rate of
 273 dilation after the deviatoric stress peak, which is one of the key features of structured soils.

274 The framework chosen for the softening case appears suitable and very powerful. The assumptions made
 275 to calculate automatically in the background the parameters $p_{y,s}^{\Pi}$ and β_s (Figure 12) are therefore relevant
 276 and successful to reproduce the majority of the main features of behaviour of lime treated soils, and that
 277 using only information from isotropic test results. It also ensures that the material experiences dilation at
 278 yield for samples in the dry side.

279 The MLTS appears very satisfactory to model the key features of lime treated soils considering the
 280 limited number of parameters and the straightforwardness of their determination. Nevertheless, the model

281 tends to deviate from the experimental results during the post-yield stage before converging back toward
282 the critical state at high axial strains for some samples subjected to a high preconsolidation pressure (600
283 kPa in Figure 15, 900 kPa in Figure 16). In this model, potentials f and g are associated and hardening
284 is controlled by the plastic volumetric deformations ε_p^p only ($f(\boldsymbol{\sigma}, \varepsilon_p^p)$). This has for consequences to reflect
285 the degradation of the structure on the deviatoric stress. However, lime treated specimens experiencing
286 hardening do not show any sign of this phenomenon for any of the concentrations tested. This might come
287 from the fact that the contribution of ε_q^p was neglected in this model, and/or that the ‘amount’ of structure
288 is too low to significantly affect the stresses.

289 For samples in the dry side, the model predicts larger values for the yield loci than what is experimentally
290 observed. One of the known limitations of the MCC is that it overestimates the values in such situation;
291 the fact that we extended the yield function in the tensile domain with p_b amplifies this feature.

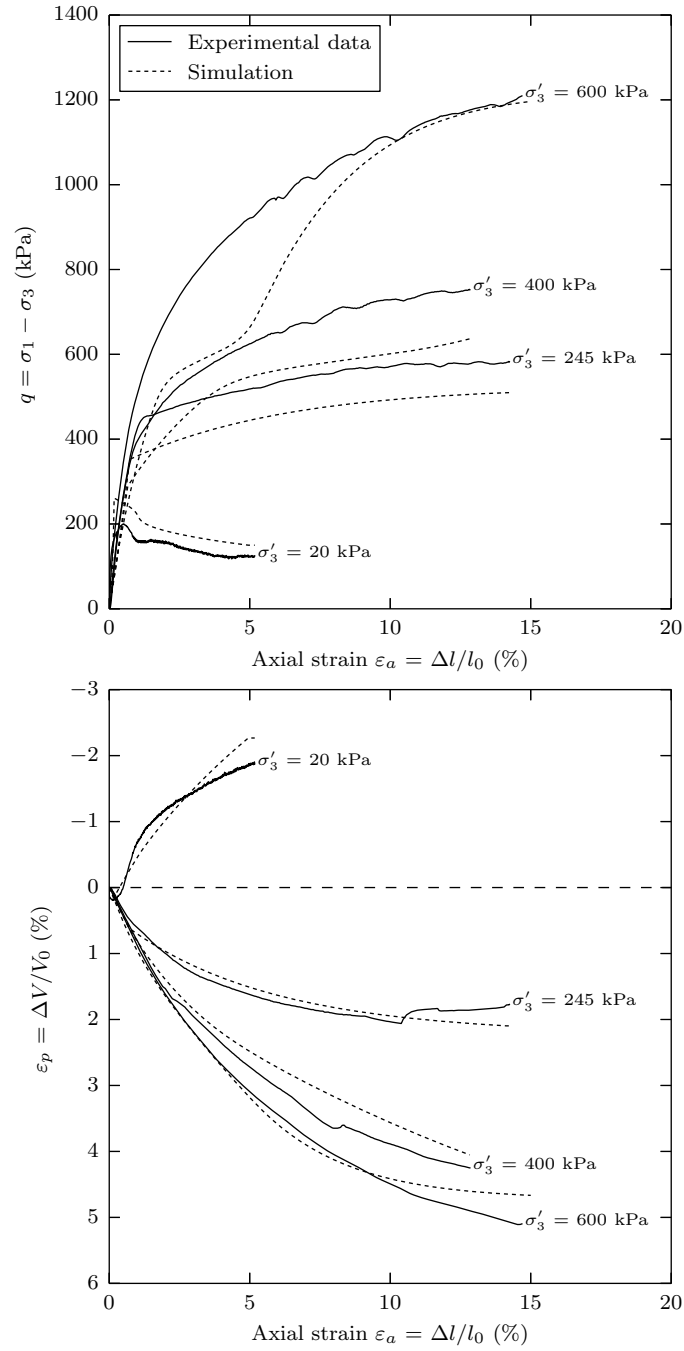


Figure 15: Comparison between experimental results and the model of drained triaxial tests performed on lime treated specimens with 1% CaO (Robin et al., 2014a).

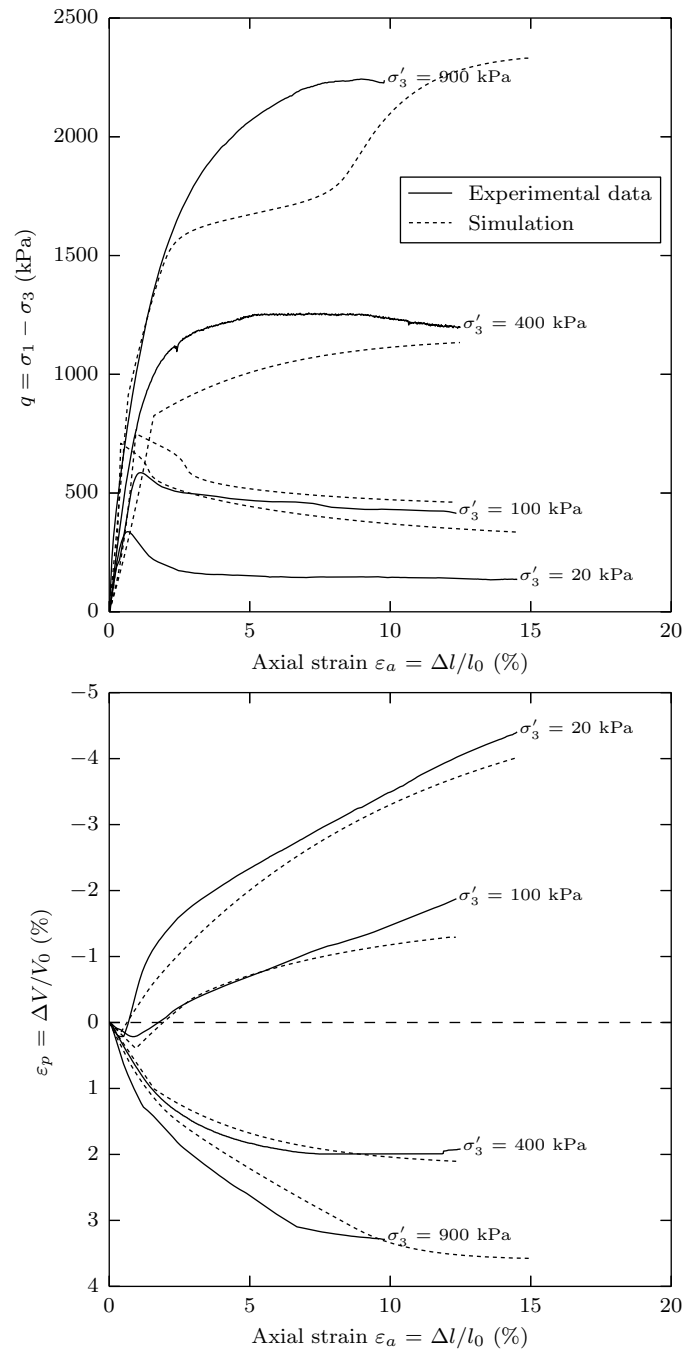


Figure 16: Comparison between experimental results and the model of drained triaxial tests performed on lime treated specimens with 2% CaO (Robin et al., 2014a).

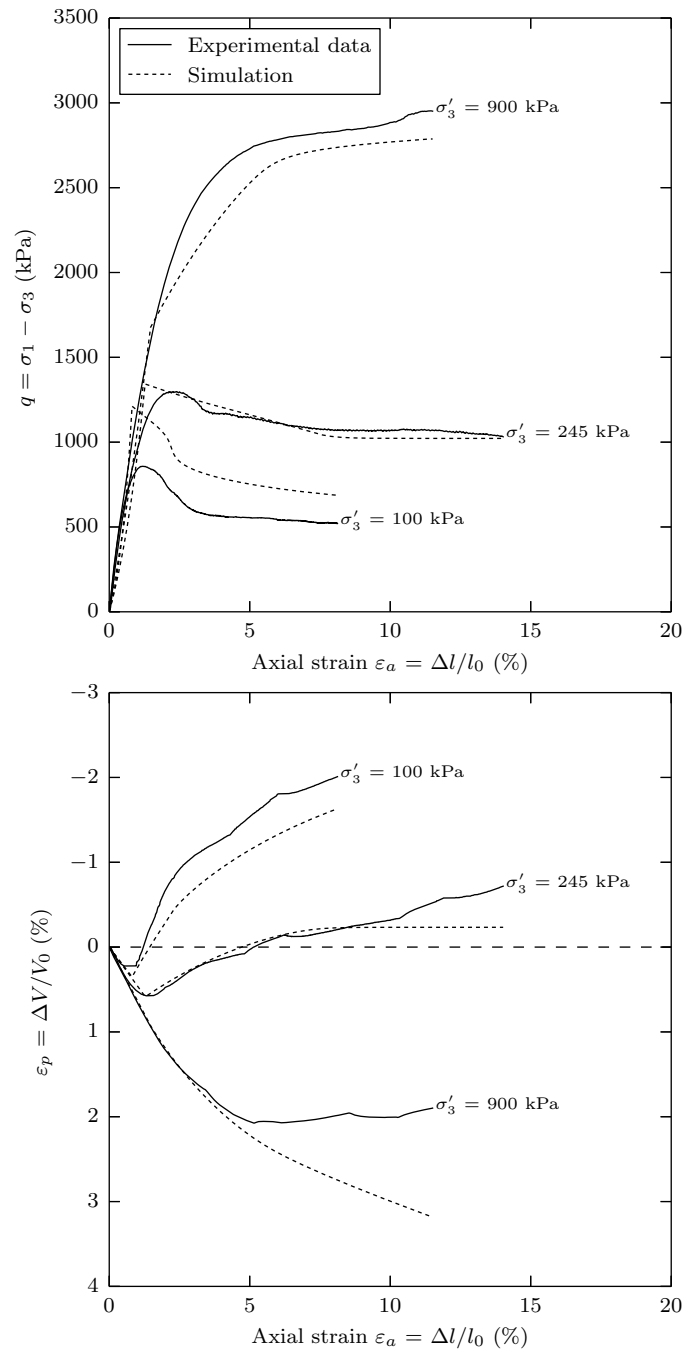


Figure 17: Comparison between experimental results and the model of drained triaxial tests performed on lime treated specimens with 5% CaO (Robin et al., 2014a).

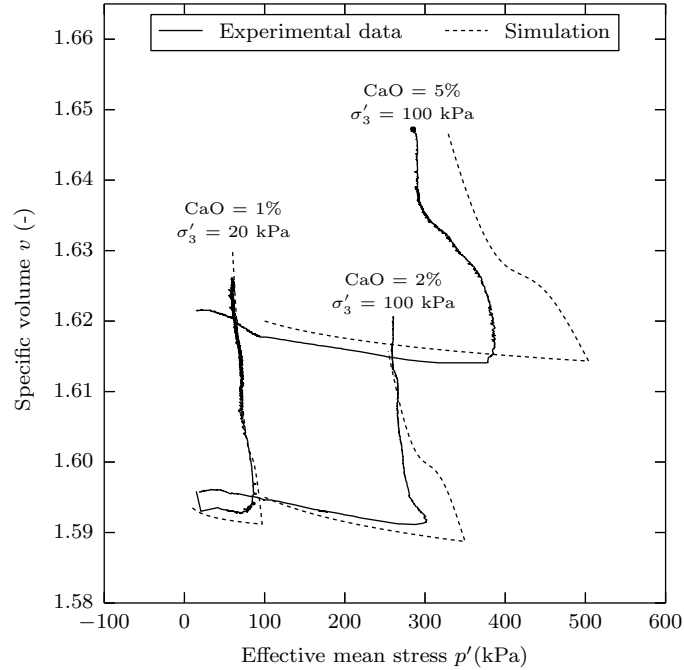


Figure 18: Comparison between drained triaxial results and the model of the specific volume for different lime contents (Robin et al., 2014a).

292 5.3. Naturally structured soils

293 Although the formulation was originally designed for lime treated soils, there are several common features
 294 of behaviour between artificially and naturally materials that could also make it suitable for the latter.

295 5.3.1. Isotropic consolidation

296 The suitability of the formulation to model the degradation of naturally structured soils under isotropic
 297 loading is verified using the results from Lagioia and Nova (1995) on natural calcarenite (Figure 19). Likewise
 298 the lime treated specimens, calcarenite experiences a degradation of the structure at yield but that occurs
 299 immediately at yield ($p_y^I = p_y^{II}$) and at a very high rate. Again, β was solved numerically using the Newton-
 300 Raphson procedure. There is no information about the behaviour of the destructured calcarenite under
 301 isotropic loading, and therefore no information is given about the value of the residual void ratio Δe_c .
 302 However, Lagioia and Nova (1995) considered that calcarenite converges toward the ncl of the destructured
 303 state. Thus, it is assumed that calcarenite has no residual void ratio ($\Delta e_c = 0$) and follows the mode 1.
 304 The parameters used for the simulations are given in Table 3.

305 Though the origin of the cementation is different, the MLTS appears suitable to model naturally struc-
 306 tured materials under isotropic loading. As for the lime treated specimens, the degradation is initiated at
 307 the right effective mean stress and at the correct rate till it reaches the normal compression line of the
 308 destructured state.

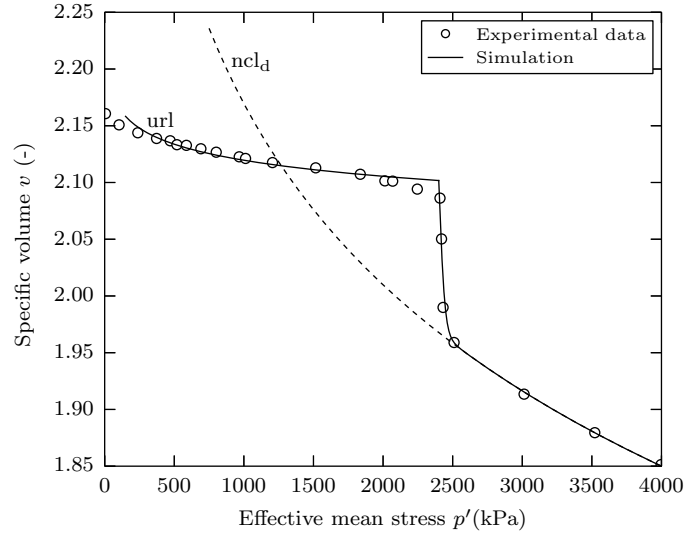


Figure 19: Validation of the formulation on natural calcarenite (after [Lagioia and Nova \(1995\)](#)) – ncl: normal compression line.

309 5.3.2. Shear behaviour

310 The model is now tried to reproduce the behaviour of samples naturally structured calcarenite at shear
 311 submitted to drained triaxial tests. The parameter p_b was determined from the equation of CSL given in
 312 [Lagioia and Nova \(1995\)](#).

313 For samples of calcarenite experiencing hardening ([Figure 20](#)) the MLTS gives a very good agreement
 314 with the experimental results of the yield loci and the convergence toward the critical state. At yield, the
 315 degradation of the structure seems to affect the deviatoric stress, which is successfully described by model.
 316 The specific volume at yield ([Figure 21](#)) is accurately modelled and the trends of the volumetric deformations
 317 ([Figure 20](#)) are satisfactory, although the values appear underestimated at large deformations.

318 For samples experiencing softening ([Figure 22](#)) the MLTS gives an accurate prediction of the yield loci
 319 and the convergence toward the critical state. However, samples revealed an unusual behaviour in the
 320 framework of the MCC and the critical state theory regarding the volumetric deformations. It is generally
 321 accepted that for the softening case samples experience dilation at yield. However, the calcarenite seems to
 322 behave differently and keeps contracting at yield, although the deviatoric stress decreases.

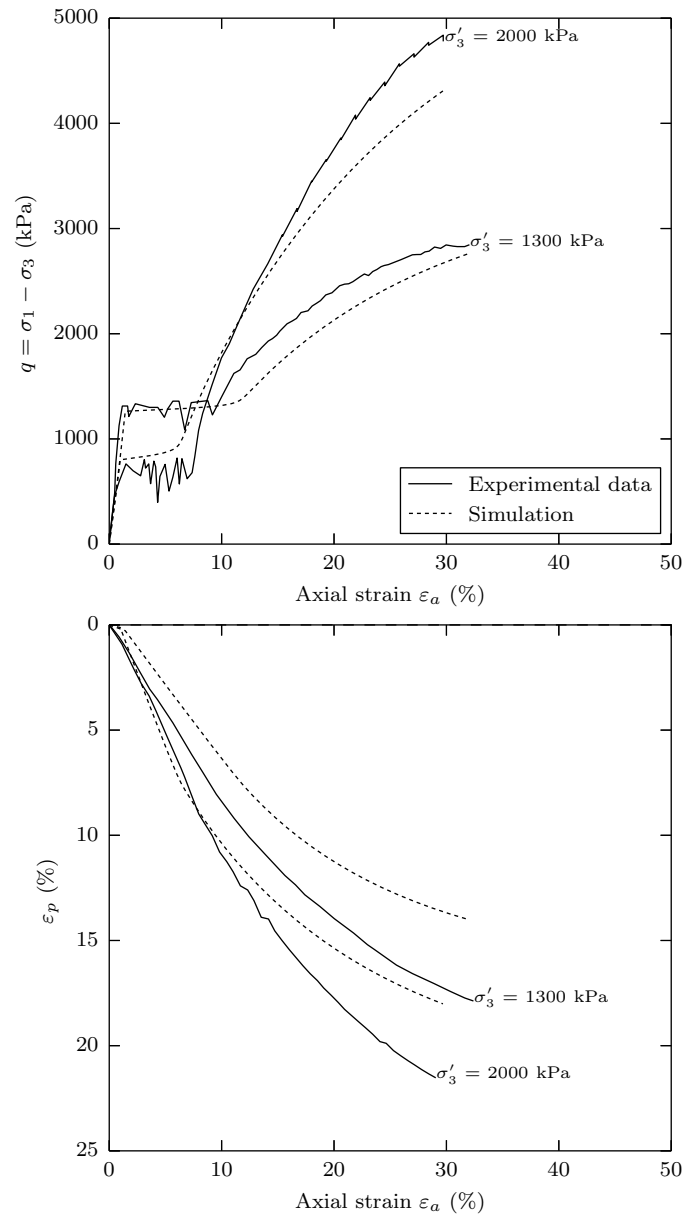


Figure 20: Comparison between experimental results and the model of drained triaxial tests performed on calcarenite and experiencing hardening (Lagioia and Nova, 1995).

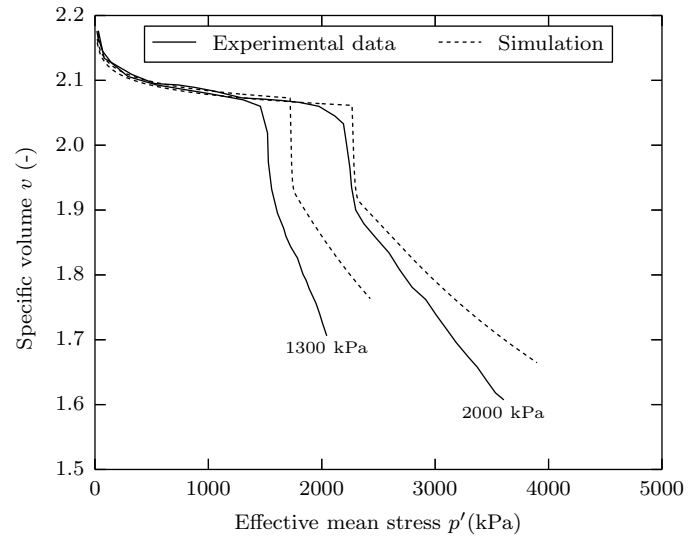


Figure 21: Comparison between the experimental results and the model for the specific volume (Lagioia and Nova, 1995)

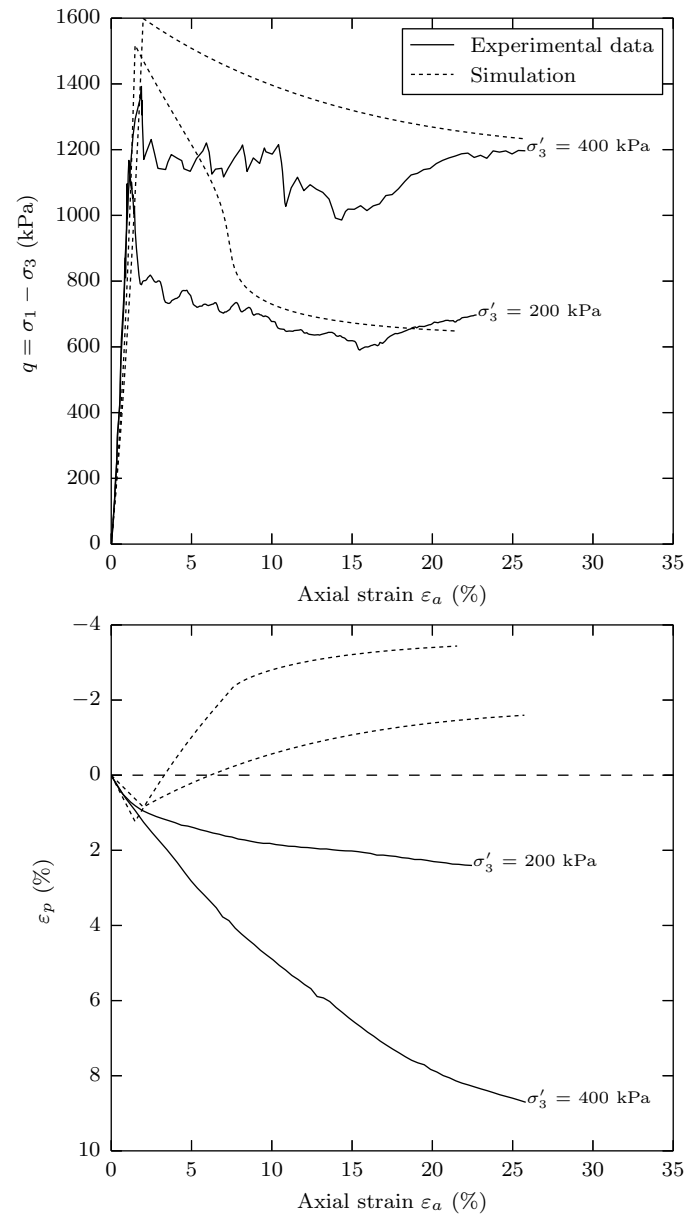


Figure 22: Comparison between experimental results and the model of drained triaxial tests performed on calcarenite and experiencing softening (Lagioia and Nova, 1995).

323 *5.4. Discussion: influence of the initial void ratio on the degradation mode*

324 The MLTS can successfully reproduce a large number of features of both lime treated soils and naturally
325 structured soils. However, the model deviates from the experimental results for 1) lime treated specimens
326 subjected to high preconsolidation pressures experiencing hardening, and 2) samples of calcarenite experi-
327 encing softening. In this section, we propose a hypothesis to explain these limitations using the initial void
328 ratio of the material.

329 During the early post-yield stage, the degradation of the structure seems to affect the stress:strain
330 response for samples of calcarenite experiencing hardening, but not for the lime treated specimens. Fur-
331 thermore, for the softening case, lime treated specimens experience dilation, as predicted by the critical
332 state theory, but this is not the case for the samples of calcarenite, which experience contraction despite the
333 decrease of deviatoric stress at yield.

334 For the calcarenite, the initial additional void ratio at yield Δe_i and the range of stresses are similar to
335 those measured on lime treated soils with 5% CaO. The only difference between the two materials lies in
336 the initial specific volume (around 1.6 for the lime treated specimens and 2.2 for the calcarenite). When
337 the calcarenite starts yielding, the structure is rapidly degraded due to the brittleness of the material.
338 [Lagioia and Nova \(1995\)](#) stated that some softening could take place under isotropic loading, and explained
339 that the plateau of the deviatoric stress is associated with debonding. However, what was interpreted as
340 *softening* under isotropic loading is more likely to be collapse since the specific volume decreases during the
341 destructuration. Once the particles are released from the cementation, they immediately collapse and start
342 filling the voids as the axial deformation increases. During this stage, there is no effective friction inside the
343 material and therefore no additional deviatoric stress is necessary to increase the axial deformation. The
344 effective friction is restored once the particles are close enough and the porosity is significantly reduced,
345 which leads to an increase of the deviatoric stress followed by convergence toward the critical state. This
346 mechanism also explains why samples experiencing softening do not have a dilatant behaviour at yield as
347 predicted by the critical state theory. The dilation process is the direct result of the interlocking of the
348 particles; in the case of the calcarenite, the fast degradation of the structure leads to the collapsing of the
349 particles and therefore to the contraction of the sample. Although the deviatoric stress decreases at yield,
350 since there is no interlocking of the particles, there is no dilation of the sample.

351 For the lime treated specimens of this study, the initial conditions were chosen to match those used
352 on-site and obtained from the Proctor compaction test ([Robin et al., 2014a](#)). In these conditions, the void
353 ratio is too low to generate a noticeable collapse in the material, and the destructuration is a slower process.
354 The degradation of the structure takes place but particles are already in contact, which maintains a friction
355 between them and leads to increase in the deviatoric stress with the axial deformation. Therefore, the
356 degradation of the structure is not observed directly on the stress:strain response. If the conditions imply
357 strain softening, interlocking happens and therefore dilation, which is observed on the experimental results

358 and properly reproduced by the MLTS.

359 In light of these observations, it appears that the initial void ratio has a higher impact on the behaviour
 360 of the material than the degree and the origin of cementation. As matter of fact, the mode of degradation of
 361 a large number of structured materials seems to be closely related to the initial void ratio (Table 4). Further
 362 work must be carried out to identify the parameters responsible for the different behaviours. Nevertheless,
 363 the MLTS appears to reproduce the main features of behaviour of lime treated soils, and is also successful
 364 in modelling the main trends that are observed in naturally structured soils.

Table 4: Correlation between the initial void ratio and the mode of degradation

	Origin of structure	Material	v_i (-)	Study
Mode 1	Natural	Pisa clay	2.8	Callisto and Calabresi (1998)
	Artificial	St-Alban clay	6.0	Tremblay et al. (2001)
Mode 2	Natural	Louiseville clay	3.0	Lapierre et al. (1990)
	Artificial	Louiseville clay	$\gg 3$	Tremblay et al. (2001)
Mode 3	Natural	Corinth marl	1.6	Anagnostopoulos et al. (1991)
	Artificial	Silt	1.6	Robin et al. (2014a)
Mode 4	Natural	Vallericca clay	1.8	Callisto and Rampello (2004)
	Artificial	Sandstone	<1.6	Rotta et al. (2003)

v_i : initial specific volume.

365 6. Conclusion

366 A new model in the framework of the Modified Cam Clay model was developed for lime treated soils.
 367 In order to introduce only relevant parameters, the most important features of lime treated materials and
 368 naturally structured soils that should be reproduced by a model were identified. Experimental results reveal
 369 that both naturally and artificially cemented soils have a very similar mechanical behaviour at yield.

370 To account for the effects of structure on the behaviour of soils, a new formulation was developed based
 371 on Richards's equation. Only 4 new additional parameters to the MCC were introduced: the degradation
 372 stress p_y^{II} , the rate of degradation β , the additional void ratio at p_y^{I} , and the additional void ratio Δe_c at
 373 $p' \rightarrow +\infty$. The power of this model is that all the additional parameters have a physical meaning and can be
 374 determined from a single isotropic consolidation test performed on the structured material. A transparent

375 and powerful procedure was developed for the softening rule. The two parameters required by the sigmoid
376 function to model the degradation are automatically determined from the 4 parameters obtained from the
377 isotropic tests.

378 The model was applied for lime treated soils and naturally structured samples of calcarenite. The
379 formulation is in good agreement with the experimental results and the main trends are properly reproduced.
380 The formulation proposed as softening rule is successful to model the dilation observed on lime treated
381 samples at yield and the maximum rate of dilation after the peak, one of the most representative features
382 of structured soils. However, the results on the calcarenite have risen interesting considerations for the
383 modelling of the structured materials in general, naturally or artificially.

384 The initial porosity appeared to be the key parameter controlling the influence of the mode of structure
385 degradation on the mechanical behaviour of lime treated specimens and the calcarenite. Once the material
386 starts yielding the degradation of the bonding structure takes place, and therefore the release of the particles.
387 Depending on the initial void ratio, the material can either experience dilation (particles are in contact and
388 expand due to the interlocking) or collapse until particles start interacting again. This can lead to reduction
389 of volume even for heavily over consolidated samples.

390 Further work must be carried out to develop a model capable of accounting for the influence of the initial
391 void ratio on the post-yield behaviour.

392 **Appendix A. Notation**

Symbol	Definition
CSL	Critical State Line
E	Young's modulus
f	yield function
g	plastic potential
G	shear modulus
M	slope of critical state line
MCC	Modified Cam Clay Model
MLTS	Model for Lime Treated Soils
ncl	normal compression line
ncl _d	normal compression line of the destructured state
ncl _r	normal compression line of the residual state

Symbol	Definition
ncl_{mcc}	normal compression line of modified Cam Clay model
N_λ	specific volume at $p' = 1$ kPa
p'	effective mean stress
p_b	tensile stress
p_y^I	primary yield stress
p_y^{II}	degradation stress
$p_{y,s}^{II}$	degradation stress for softening case
q	deviatoric stress
url	unloading-reloading line
v	specific volume
v_s	specific volume for the structured soil
α	parameter of bijection for softening case
β	rate of degradation
β_s	rate of degradation for softening case
β_0	rate of degradation for monotonic decreasing function v_s
Δe_c	residual additional void ratio at $p' \rightarrow +\infty$
Δe_i	initial additional void ratio at $p' = p_y^I$
$\varepsilon_p, \varepsilon_p^e, \varepsilon_p^p$	total, elastic, and plastic volumetric strains
$\varepsilon_q, \varepsilon_q^e, \varepsilon_q^p$	total, elastic, and plastic deviatoric strains
κ	elastic stiffness parameter for changes in effective mean stress
λ	plastic stiffness parameter for changes in effective mean stress
ξ	gradient of the curve ($v : p'$) at $p' = p_y^{II}$
σ_1, σ_3	axial, radial stress

7. References

- Ahnberg, H., 2007. On yield stresses and the influence of curing stresses on stress paths and strength measured in triaxial testing of stabilized soils. *Canadian geotechnical journal* 44 (1), 54–66.
- Anagnostopoulos, a. G., Kalteziotis, N., Tsiambaos, G. K., Kavvas, M., 1991. Geotechnical properties of the Corinth Canal marls. *Geotechnical and Geological Engineering* 9 (1), 1–26.
- Aversa, S., 1991. Mechanical behaviour of soft rocks: some remarks. In: *Proc. of the Workshop on "Experimental characterization and modelling of soils and soft"*. Vol. 98. pp. 191–223.
- Balasubramaniam, A., Buessuesco, B., Oh, Y.-N. E., Bolton, M. W., Bergado, D., Lorenzo, G., 2005. Strength degradation and critical state seeking behaviour of lime treated soft clay. In: *International Conference on Deep Mixing-Best Practice and Recent Advances*. Vol. 1. Stockholm, pp. 35–40.
- Baudet, B., Stallebrass, S., 2004. A constitutive model for structured clays. *Géotechnique* 54 (4), 269–278.
- Brandl, H., 1981. Alteration of soil parameters by stabilization with lime. In: *10th International Conference on Soil Mechanics and Foundation Engineering*. Stockholm, pp. 587–594.
- Burland, J. B., 1990. On the compressibility and shear strength of natural clays. *Géotechnique* 40 (3), 329–378.
- Burland, J. B., Rampello, S., Georgiannou, V. N., Calabresi, G., 1996. A laboratory study of the strength of four stiff clays. *Géotechnique* 46 (3), 491–514.
- Callisto, L., Calabresi, G., 1998. Mechanical behaviour of a natural soft clay. *Géotechnique* 48 (4), 495–513.
- Callisto, L., Rampello, S., 2004. An interpretation of structural degradation for three natural clays. *Canadian Geotechnical Journal* 41 (3), 392–407.
- Consoli, N. C., Lopes, L. d. S., Prietto, P. D. M., Festugato, L., Cruz, R. C., 2011. Variables Controlling Stiffness and Strength of Lime-Stabilized Soils. *Journal of Geotechnical and Geoenvironmental Engineering* 137 (6), 628–632.
- Corless, R. M., Gonnet, G. H., Hare, D. E. G., Jeffrey, D. J., Knuth, D. E., 1996. On the Lambert W Function. *Advances in Computational Mathematics* 5, 329–359.
- Cotecchia, F., Chandler, R. J., 2000. A general framework for the mechanical behaviour of clays. *Géotechnique* 50 (4), 431–447.
- Cuisinier, O., Auriol, J.-C., Le Borgne, T., Deneele, D., 2011. Microstructure and hydraulic conductivity of a compacted lime-treated soil. *Engineering Geology* 123 (3), 187–193.
- Cuisinier, O., Masrouri, F., Pelletier, M., Villieras, F., Mosser-Ruck, R., 2008. Microstructure of a compacted soil submitted to an alkaline PLUME. *Applied Clay Science* 40 (1-4), 159–170.
- Flora, A., Lirer, S., Amorosi, A., Elia, G., 2006. Experimental observations and theoretical interpretation of the mechanical behaviour of a grouted pyroclastic silty sand. In: *Proc. VI European Conference on Numerical Methods in Geotechnical Engineering, NUMGE 06*. Graz, Austria.
- Gens, A., Nova, R., 1993. Conceptual bases for a constitutive model for bonded soils and weak rocks. *Geotechnical engineering of hard soils-soft rocks* 1 (1), 485–494.
- Horpibulsuk, S., Liu, M. D., Liyanapathirana, D. S., Suebsuk, J., 2010. Behaviour of cemented clay simulated via the theoretical framework of the Structured Cam Clay model. *Computers and Geotechnics* 37 (1-2), 1–9.
- Kavvas, M., Amorosi, A., 2000. A constitutive model for structured soils. *Géotechnique* 50 (3), 263–273.
- Lagioia, R., Nova, R., 1995. An experimental and theoretical study of the behaviour of a calcarenite in triaxial compression. *Géotechnique* 45 (4), 633–648.
- Lapierre, C., Leroueil, S., Locat, J., 1990. Mercury intrusion and permeability of Louiseville clay. *Canadian Geotechnical Journal* 27 (6), 761–773.
- Leroueil, S., Vaughan, P. R., 1990. The general and congruent effects of structure in natural soils and weak rocks. *Géotechnique* 40 (3), 467–488.
- Little, D. N., 1995. *Stabilization of pavement subgrades and base courses with lime*. Kendall Hunt Pub Co.

436 Liu, M. D., Carter, J. P., 2002. A structured Cam Clay model. *Canadian Geotechnical Journal* 39 (6), 1313–1332.

437 Liu, M. D., Carter, J. P., 2003. Volumetric Deformation of Natural Clays. *International Journal of Geomechanics* 3 (2), 236–252.

438 Maccarini, M., 1987. Laboratory studies for a weakly bonded artificial soil. Ph.D. thesis, Imperial College London (University
439 of London).

440 Malandraki, V., Toll, D. G., 2001. Triaxial Tests on Weakly Bonded Soil with Changes in Stress Path. *Journal of Geotechnical
441 and Geoenvironmental Engineering* 127 (3), 282–291.

442 Muir Wood, D., 2004. *Geotechnical modelling*. Vol. Applied Ge. CRC Press.

443 Nguyen, L. D., Fatahi, B., Khabbaz, H., 2014. A constitutive model for cemented clays capturing cementation degradation.
444 *International Journal of Plasticity* 56, 1–18.

445 Nova, R., Castellanza, R., Tamagnini, C., 2003. A constitutive model for bonded geomaterials subject to mechanical and/or
446 chemical degradation. *International journal for numerical and analytical methods in geomechanics* 27 (9), 705–732.

447 Oliveira, P. V., 2013. Effect of Stress Level and Binder Composition on Secondary Compression of an Artificially Stabilized
448 Soil. *Journal of Geotechnical and Geoenvironmental Engineering* 139 (5), 810–820.

449 Rampello, S., Callisto, L., 1998. A study on the subsoil of the Tower of Pisa based on results from standard and high-quality
450 samples. *Canadian Geotechnical Journal* 35 (6), 1074–1092.

451 Richards, F., 1959. A flexible growth function for empirical use. *Journal of experimental Botany* 10 (29), 290–300.

452 Robin, V., Cuisinier, O., Masrouri, F., Javadi, A. A., 2014a. Chemo-mechanical modelling of lime treated soils. *Applied Clay
453 Science* 95, 211–219.

454 Robin, V., Javadi, A. A., Cuisinier, O., Masrouri, F., 2014b. A new formulation to model the degradation in structured soils.
455 In: *8th European Conference on Numerical Methods in Geotechnical Engineering*. Delft, pp. 97–102.

456 Roscoe, K. H., Burland, J. B., 1968. On the generalized stress-strain behaviour of wet clay. *Engineering Plasticity*, 535–609.

457 Rotta, G. V., Consoli, N. C., Prietto, P. D. M., Coop, M. R., Graham, J., 2003. Isotropic yielding in an artificially cemented
458 soil cured under stress. *Géotechnique* 53 (5), 493–501.

459 Rouainia, M., Muir wood, D., 2000. A kinematic hardening constitutive model for natural clays with loss of structure.

460 Suebsuk, J., Horpibulsuk, S., Liu, M. D., 2010. Modified Structured Cam Clay: A generalised critical state model for destruc-
461 tured, naturally structured and artificially structured clays. *Computers and Geotechnics* 37 (7-8), 956–968.

462 Suebsuk, J., Horpibulsuk, S., Liu, M. D., 2011. A critical state model for overconsolidated structured clays. *Computers and
463 Geotechnics* 38 (5), 648–658.

464 Tremblay, H., Leroueil, S., Locat, J., 2001. Mechanical improvement and vertical yield stress prediction of clayey soils from
465 eastern Canada treated with lime or cement. *Canadian Geotechnical Journal* 38 (3), 567–579.

466 Vatsala, A., Nova, R., Srinivasa Murthy, B. R., 2001. Elastoplastic Model for Cemented Soils. *Journal of Geotechnical and
467 Geoenvironmental Engineering* 127 (8), 679–687.

468 Wissa, A. E., Ladd, C. C., Lambe, T. W., 1965. Effective stress strength parameters of stabilized soils. In: *International
469 conference on soil mechanics and foundation engineering*. Montréal, pp. 412–416.

470 Yang, C., Carter, J. P., Sheng, D., 2014. Description of compression behaviour of structured soils and its application 933 (July
471 2013), 921–933.

472 Yong, R., Nagaraj, T., 1977. Investigation of fabric and compressibility of a sensitive clay. In: *Proceedings of the International
473 Symposium on Soft Clay*, Asian Institute of Technology. pp. 327–333.

474 Zytynski, M., Randolph, M., Nova, R., Wroth, C., 1978. On modelling the unloading-reloading behaviour of soils. *International
475 Journal for Numerical and Analytical Methods in Geomechanics* 2 (1), 87–93.